Figure S1

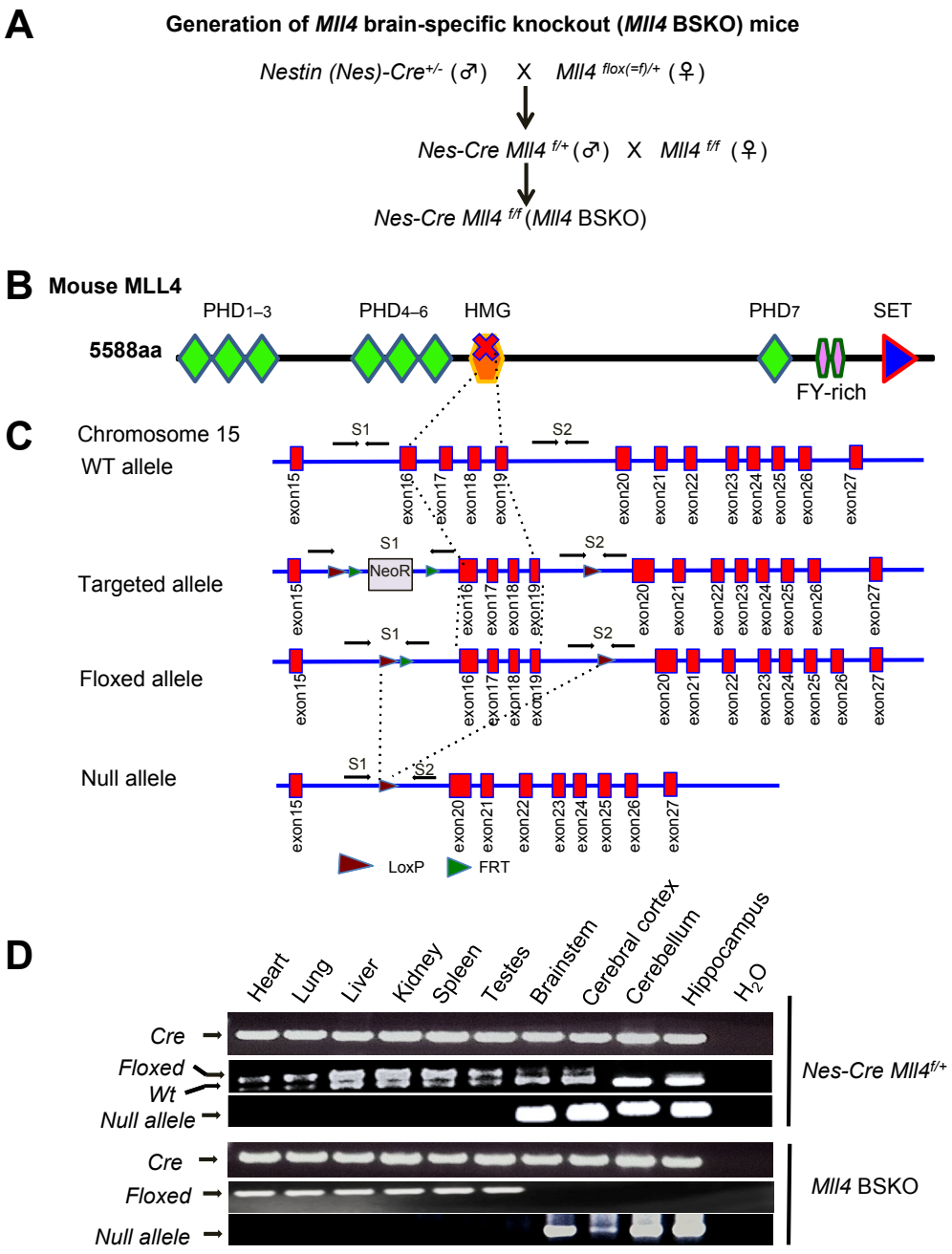

Figure S1. Generation of *Mll4* BSKO (*Nes-Cre Mll4$^{f/f}$*), related to Figure 1.

(**A**) A scheme for the generation of *Mll4* BSKO mice.

(**B**) Diagrammatic representation of the domain organization of mouse MLL4. MLL4 contains two tandem plant homeodomains (PHDs) (PHD1–3 and PHD4–6), one single PHD (PHD7), one high-mobility group (HMG), two F-Y rich domains, and the catalytic domain SET.

(**C**) The strategy for targeting the *Mll4* allele in mouse chromosome 15.

(**D**) Genotyping results using specific primers showed the generation of *Mll4* BSKO mice. *Nes, Nestin.*

Figure S2

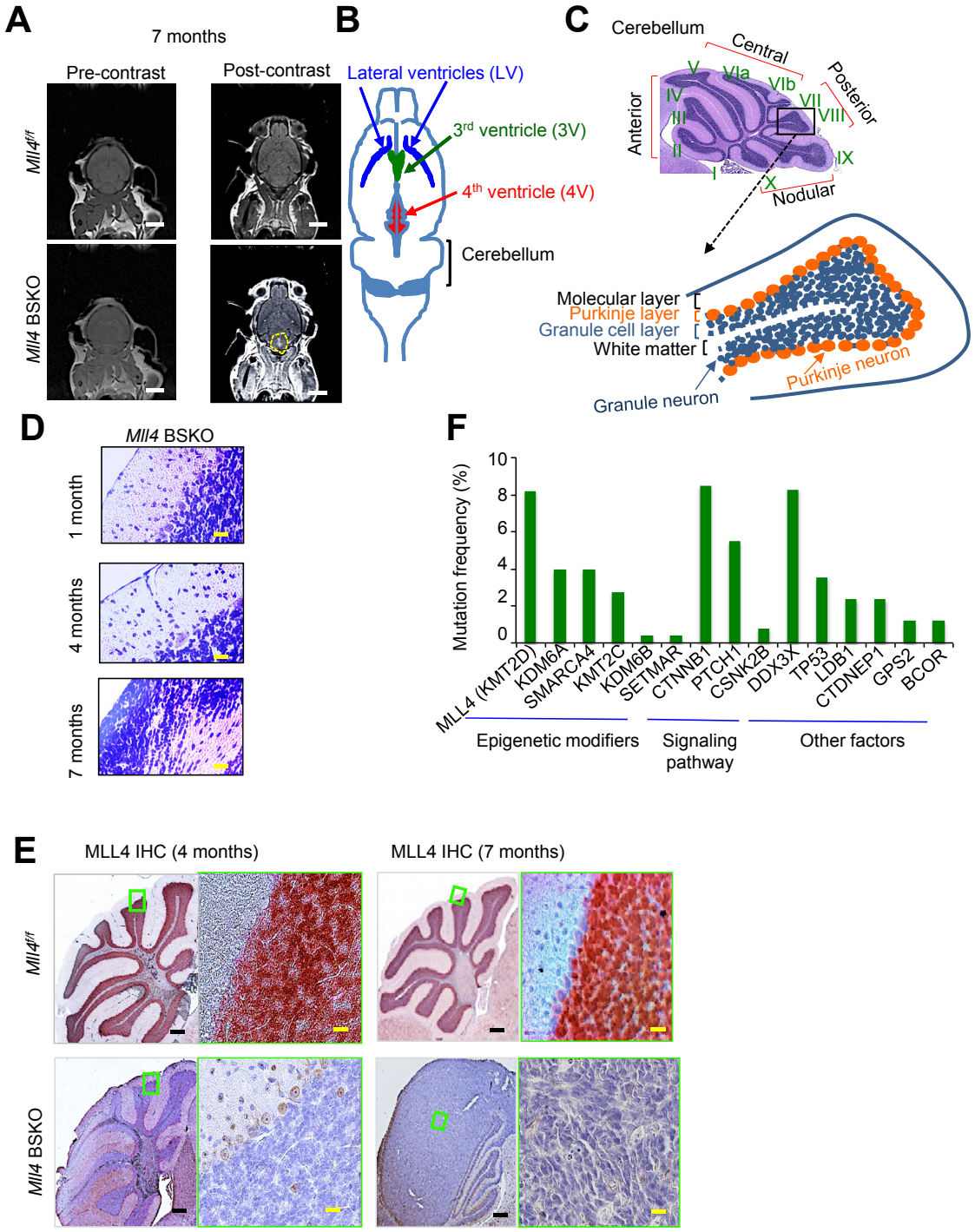

Figure S2. *Mll4* loss causes medulloblastoma (MB) in the cerebellum, related to **Figure 1.**

(**A**) T1-weighted horizontal magnetic resonance images showed a lesion in the cerebellum in *Mll4* BSKO mice (7-month-old). Yellow dotted line denotes the presence of the contrast agent Magnevist in the cerebellum in *Mll4* BSKO mice. Pre-contrast images indicate images prior to injection of Magnevist (**Left panels**). Post-contrast images indicate images after Magnevist injection (**Right panels**). Magnevist visualizes lesions and tumors by leaking out in the brain regions where blood brain barrier is compromised. White scale bars, 0.25 mm.

(**B**) A schematic illustration of a horizontal section of mouse brain.

(**C**) An enlarged picture of a sagittal section of mouse cerebellum and a schematic illustration of a cerebellar lobule in mouse cerebellum. There are ten lobules in the cerebellum.

(**D**) H&E staining of cerebellar sections in 1-, 4- and 7-month-old *Mll4* BSKO. Yellow bars, 40 μm.

(**E**) IHC staining for MLL4 showed undetectable MLL4 expression in 4- and 7-month-old *Mll4* BSKO cerebella. Red color was from MLL4 IHC while blue color was from nuclei staining by hematoxylin. Black scale bars, 200 μm; yellow scale bars, 40 μm.

(**F**) Mutation frequency of genes that are frequently mutated in MB. Data from http://www.cbioportal.org/ were analyzed. For MLL4 mutation data, data from Dubuc et al. (Acta Neuropathol 2013, 125:373-384) was also included.

Figure S3

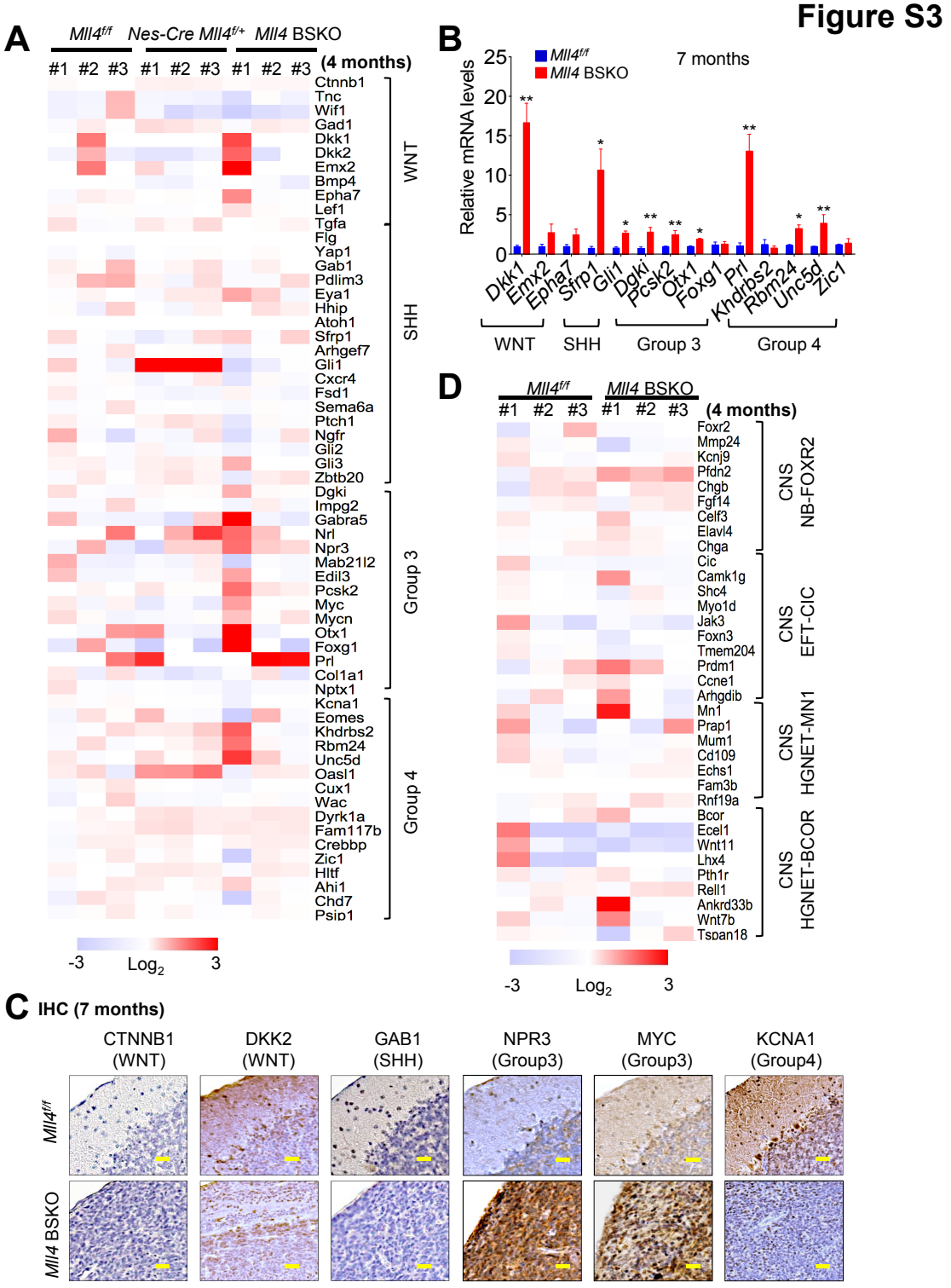

Figure S3. **Expression and IHC analysis of *Mll4* BSKO MB**, related to **Figure 3**.

(**A**) Expression levels of multiple signature genes for Group 3 were elevated in 4-month-old *Mll4* BSKO cerebella compared with control (*Mll4*$^{f/f}$) cerebella. In addition, some signature genes for other subtypes (albeit fewer than those for Group 3) were upregulated. Overall, the signature genes in expression profiles of *Mll4* BSKO cerebella #2 and #3 were much less upregulated than did those in expression profile of *Mll4* BSKO cerebellum #1. This may be because the *Mll4* BSKO cerebella #2 and #3 showed weaker cell proliferation signals than did the *Mll4* BSKO cerebellum #1 (Data not shown). RNA-Seq data of *Mll4*$^{f/f}$, *Nes-Cre Mll4*$^{f/+}$, and *Mll4* BSKO cerebella were compared to gene expression signatures of human MB subtypes (WNT, SHH, Group3, and Group 4).

(**B**) Quantitative RT-PCR results showed that signature genes for four MB subgroups, especially group 3, were upregulated in 7-month-old *Mll4* BSKO cerebella bearing MB compared with control (*Mll4*$^{f/f}$) cerebella.

(**C**) IHC analysis showed that signals of NPR3 (Group 3 marker) and MYC (Group 3 marker) were increased in 7-month-old MB-bearing *Mll4* BSKO cerebella compared with control (*Mll4*$^{f/f}$) cerebella, whereas there was no obvious difference of CTNNB1 (WNT group marker), DKK2 (WNT group marker), GAB1 (SHH group marker) and KCNA1 (Group 4 marker) signals between 7-month-old *Mll4* BSKO cerebella and control (*Mll4*$^{f/f}$) cerebella. Yellow scale bars, 40 μm.

(**D**) Expression levels of signature genes for several CNS-PNET tumors (a type of embryonal brain tumors) were not substantially changed between 4-month-old *Mll4* BSKO cerebella and control (*Mll4*$^{f/f}$) cerebella (Sturm et al., Cell, 2016).

For **A** and **D**, each column represents individual cerebellum sample, and each row corresponds to the expression value of FPKM (Fragments Per Kilo base of transcript per Million mapped reads). Gene expression levels are relative to those of control *Mll4*$^{f/f}$ cerebella in $\log_2$-fold change. Color-coded scale bars are used to indicate higher (red) and lower (purple) values than the mean values.

Figure S4

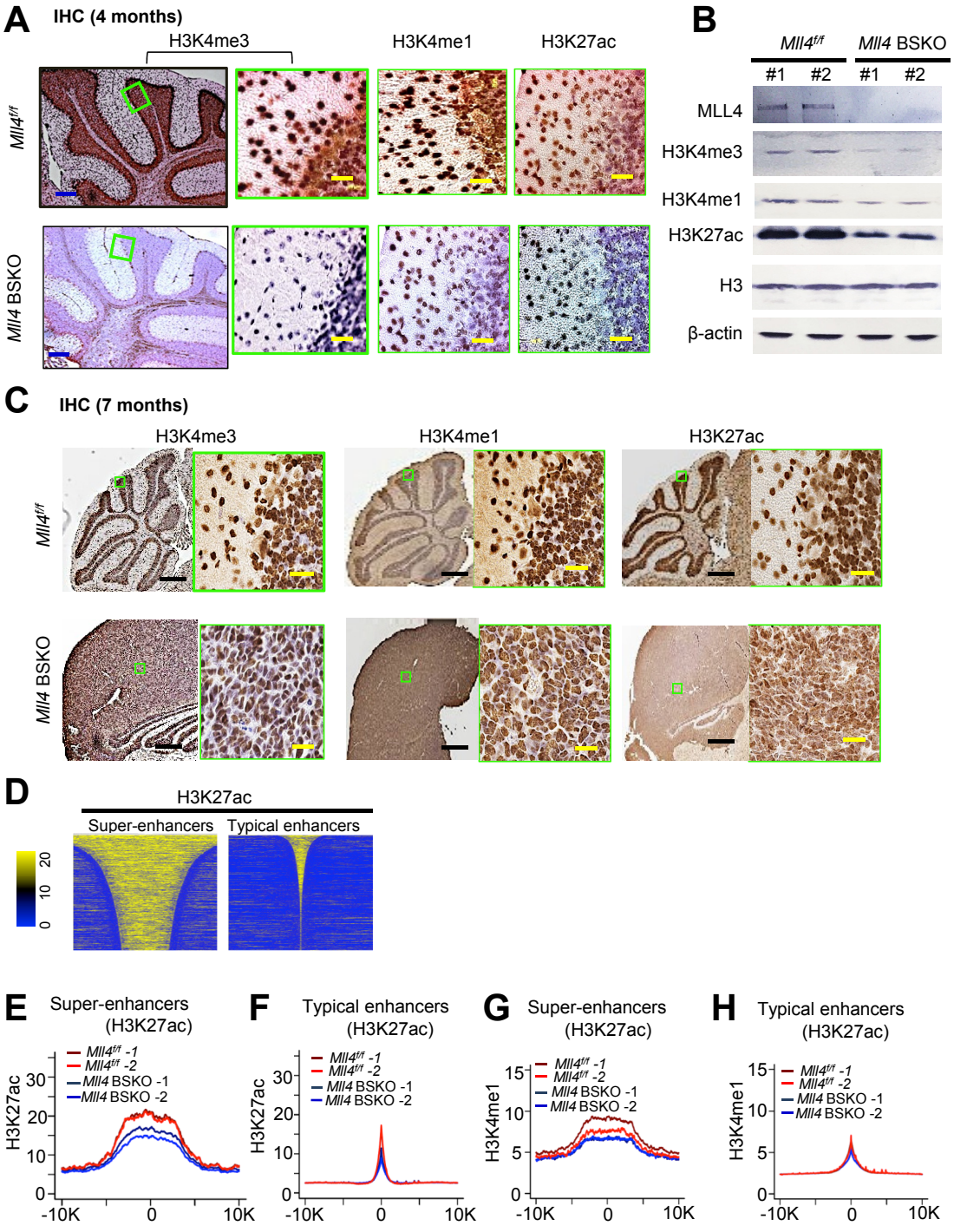

Figure S4. Analysis of H3K4me3, H3K4me1 and H3K27ac signals in *Mll4*$^{f/f}$ and *Mll4* BSKO cerebella, related to **Figure 6**

(**A**–**C**) H3K4me3, H3K4me1 and H3K27ac levels were reduced in 4-month-old *Mll4* BSKO cerebella compared with *Mll4*$^{f/f}$ cerebella but were substantially recovered in 7-month-old *Mll4* BSKO cerebella.

(**A**) IHC analysis of 4-month-old cerebella showed that H3K4me3, H3K4me1 and H3K27ac levels were decreased in *Mll4* BSKO cerebella compared with *Mll4*$^{f/f}$ cerebella.

(**B**) Western blot analysis showed that *Mll4* loss strongly reduced H3K4me3, H3K4me1 and H3K27ac levels in 4-month-old cerebella .

(**C**) IHC analysis of 7-month-old cerebella showed that H3K4me3, H3K4me1 and H3K27ac levels were not much decreased in *Mll4* BSKO cerebella compared with *Mll4*$^{f/f}$ cerebella. Black scale bars, 200 μm; Blue scale bars, 100 μm; yellow scale bars, 40 μm.

(**D**) Heat maps of super-enhancers (1,000) and typical enhancers (1,000) on the basis of H3K27ac ChIP-seq signals.

(**E**–**H**) *Mll4* loss lowered average signals of H3K27ac and H3K4me1 more in super-enhancers than in typical enhancers. Shown are average ChIP-seq read densities for H3K27ac (**E** and **F**) and H3K4me1 (**G** and **H**) at super-enhancers (**E** and **G**) and typical enhancers (**F** and **H**) from **two** *Mll4* BSKO cerebella and **two** *Mll4*$^{f/f}$ cerebella (4-month-old). Enhancers were defined using H3K27ac signals.

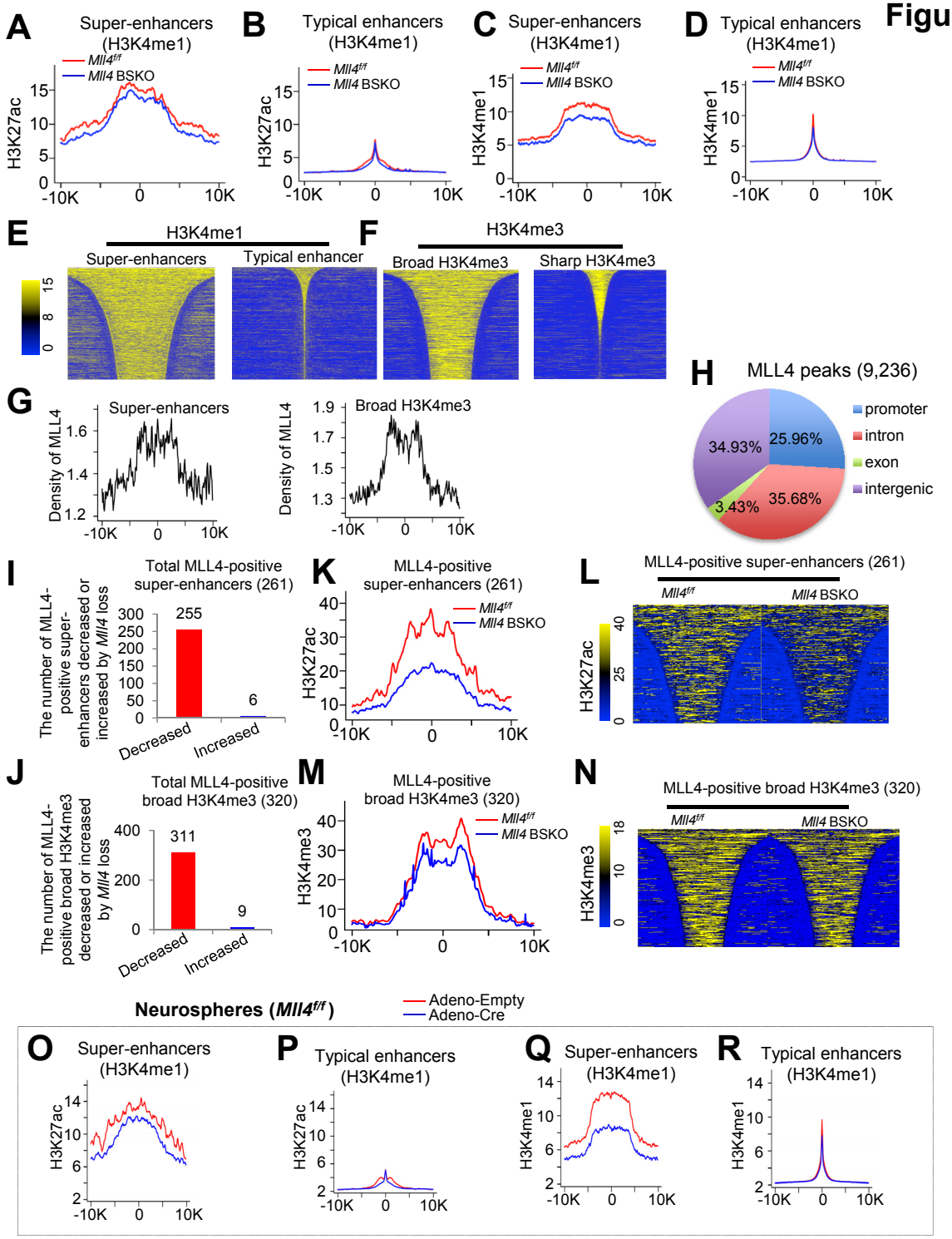

Figure S5. ***Mll4* loss results in widespread impairment of super-enhancers and broad H3K4me3 peaks**, related to **Figure 6.**

(**A**–**D**) *Mll4* loss considerably reduced average levels of H3K27ac and H3K4me1 in super-enhancers (1,000) while slightly decreasing their average levels in typical enhancers (1,000). Average ChIP-seq read densities for H3K27ac and H3K4me1 at super-enhancers and typical enhancers were compared between *Mll4*$^{f/f}$ and *Mll4* BSKO cerebella. Enhancers were defined by H3K4me1 signals. An average profile of ChIP-seq data from two *Mll4*$^{f/f}$ cerebella or two *Mll4* BSKO cerebella (4-month-old) was used to generate density plot and heat maps. Horizontal axis represents a region from −10 kb to +10 kb with the respect to the enhancer centers.

(**E**) Heat maps of super-enhancers (1,000) and typical enhancers (1,000) in mouse cerebella on the basis of H3K4me1 signals.

(**F**) Heat maps of broad H3K4me3 (1,000) and sharp H3K4me3 (1,000) peaks in mouse cerebella on the basis of H3K4me3 signals.

(**G**) Average ChIP-Seq read densities for MLL4 at 1,000 super-enhancers and 1,000 broad H3K4me3 peaks in 4-month-old *Mll4*$^{f/f}$ mice.

(**H**) The genomic distribution of ChIP-seq peaks of MLL4. ChIP-seq was performed using *Mll4*$^{f/f}$ cerebella. The MLL4 signal scale for cutoff was 8.

(**I** and **J**) Of MLL4-positive super-enhancers (261 out of 1,000) and MLL4-positive broad H3K4me3 peaks (320 out of 1,000), 255 MLL4-positive super-enhancers and 311 MLL4-positive broad H3K4me3 showed decreases in H3K27ac and H3K4me3 signals, respectively.

(**K** and **L**) Average ChIP-seq read densities (**K**) and heat maps (**L**) for super-enhancers (H3K27ac) containing MLL4 peaks in 4-month-old *Mll4*$^{f/f}$ cerebella were decreased by *Mll4* loss.

(**M** and **N**) Average ChIP-seq read densities (**M**) and heat maps (**N**) for broad H3K4me3 containing MLL4 peaks in 4-month-old *Mll4*$^{f/f}$ cerebella were decreased by *Mll4* loss.

(**O**–**R**) **In cerebellar neurospheres**, *Mll4* loss significantly decreased average levels of H3K27ac and H3K4me1 in super-enhancers (1,000) while moderately decreasing their average levels in typical enhancers (1,000). Neurospheres were isolated from *Mll4*$^{f/f}$ mouse cerebella and then treated with either Adeno-Empty or Adeno-Cre. Average ChIP-seq read densities for H3K27ac and H3K4me1 at super-enhancers and typical enhancers were compared between *Mll4*$^{f/f}$ neurospheres and *Mll4*–deleted neurospheres. Enhancers were defined by H3K4me1 signals.

Figure S6

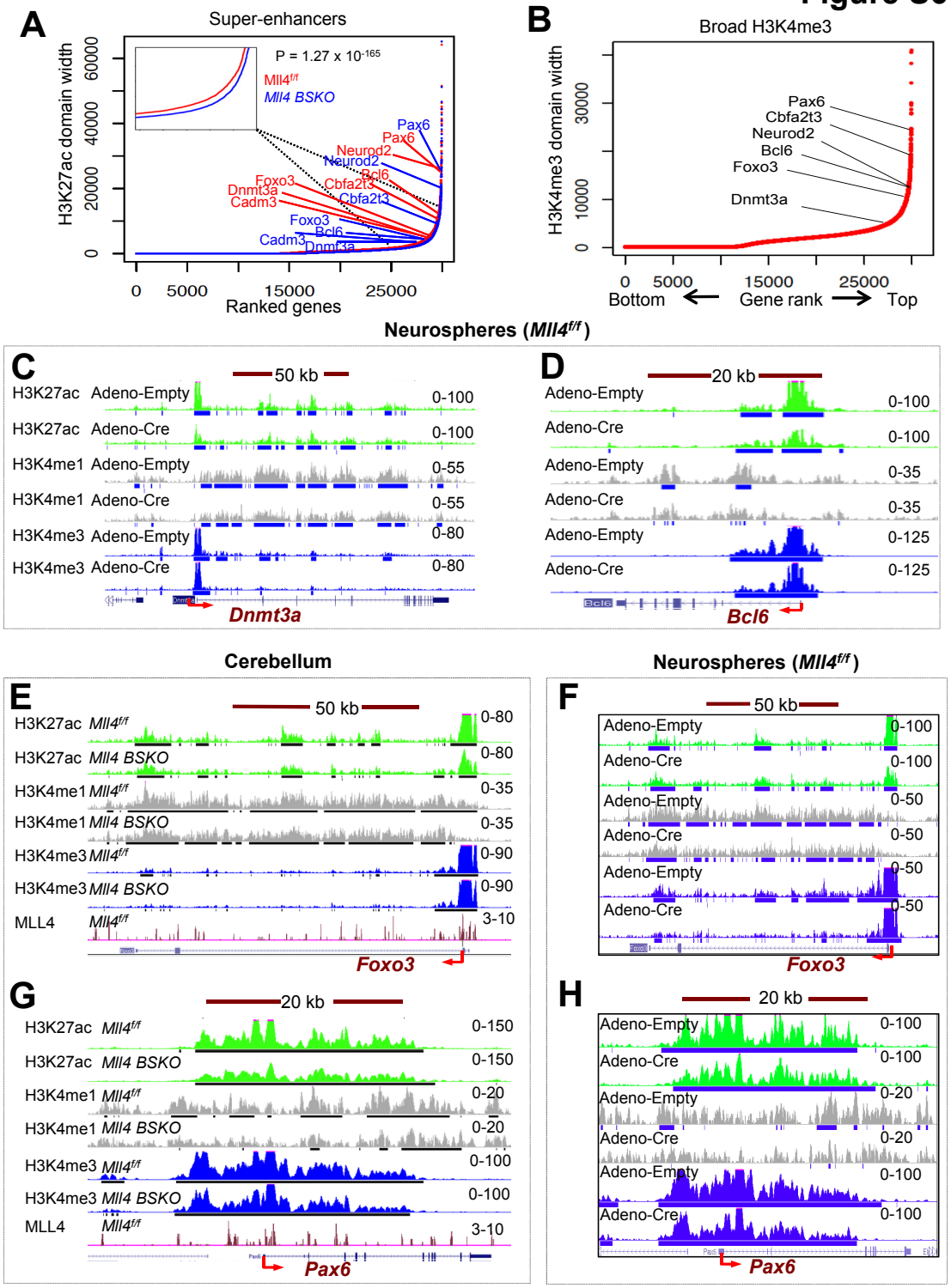

Figure S6. ***Mll4* loss reduces ChIP-seq signals of super-enhancers and broad H3K4me3 peaks that are linked to the tumor suppressor genes and neuron differentiation genes**, related to **Figure 7**.

(**A**) Plotting of H3K27ac ChIP-seq signals showed distribution of super-enhancers and enhancers in *Mll4*$^{f/f}$ and *Mll4* BSKO cerebella. Enhancer domain width was plotted on the basis of their H3K27ac signal intensity. The P value was calculated using Mann-Whitney Wilcoxon test.

(**B**) Plotting of H3K4me3 ChIP-seq signals showed distribution of broad H3K4me3 and sharp H3K4me3. H3K4me3 domain width was plotted on the basis of their H3K4me3 signal intensity.

(**C** and **D**) *Mll4* loss reduced both super-enhancer and broad H3K4me3 signals in the *Dnmt3a* and *Bcl6* genes in neurospheres. Shown are ChIP-seq profiles for H3K27ac (green), H3K4me1 (gray), and H3K4me3 (blue) at *Dnmt3a* (**C**) and *Bcl6* (**D**) genes in mouse cerebellar neurospheres treated with Adeno-Empty or Adeno-Cre.

(**E**—**H**) *Mll4* loss decreased ChIP-seq signals for H3K27ac (green), H3K4me1 (gray), H3K4me3 (blue) at the broad H3K4me3 peaks and super-enhancer regions in *Foxo3* (**E and F**), and *Pax6* (**G and H**) genes. ChIP-seq signals in mouse *Mll4 BSKO* cerebella (**E and G)** and *Mll4*-deleted neurospheres (**F and H)** were compared with those in *Mll4*$^{f/f}$ cerebella and control neurospheres, respectively. ChIP-seq signals for MLL4 are shown for *Mll4*$^{f/f}$ cerebellum. Peak tracks in the BigBed format are shown as black lines (cerebellum) and blue lines (neurospheres) under the bottom of ChIP-seq tracks.

Figure S7

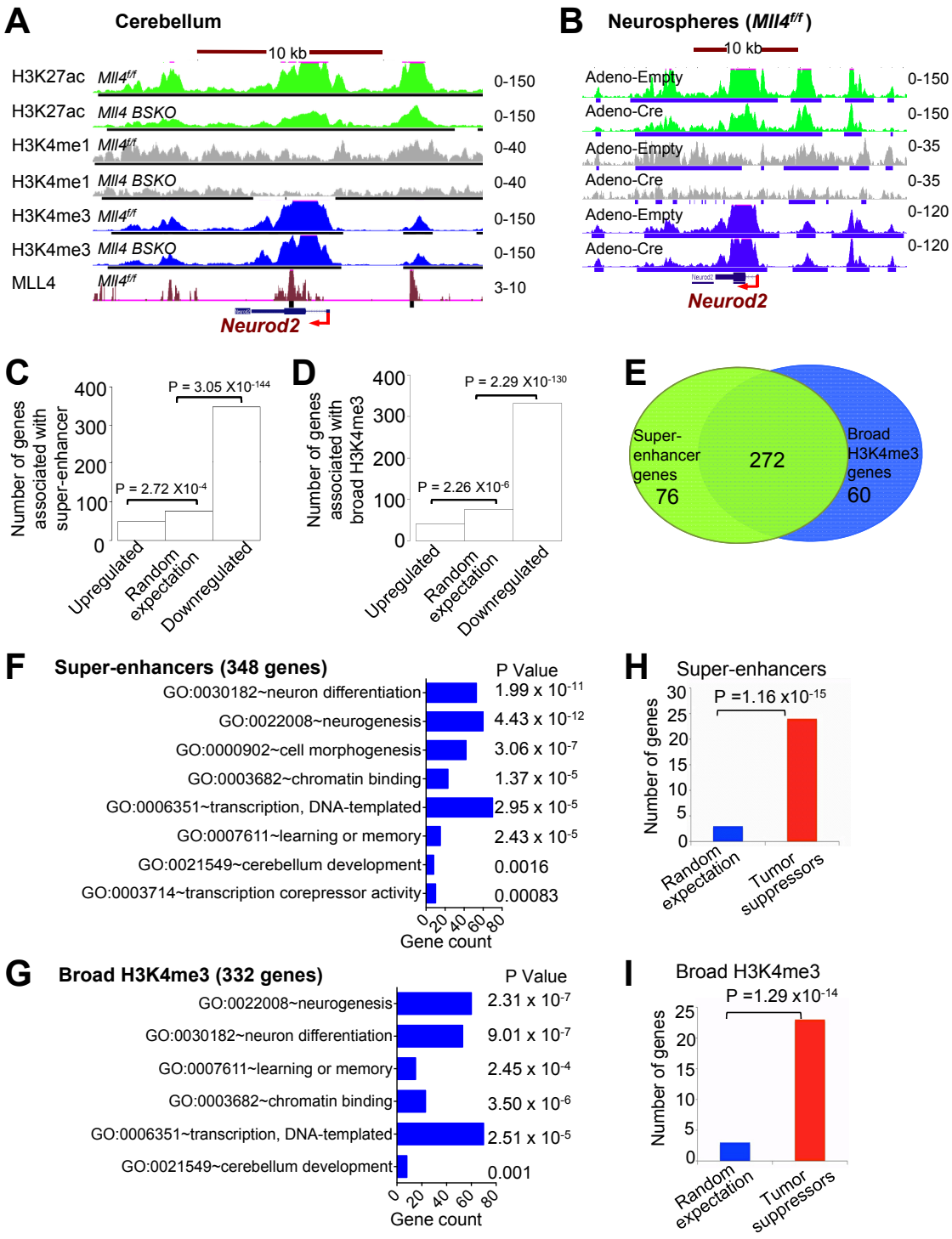

Figure S7. ***Mll4* loss downregulates tumor suppressor genes and neuron differentiation genes that are associated with super-enhancers and/or broad H3K4me3 peaks**, related to **Figure 7**.

(**A** and **B**) In both cerebella (**A**) and neurospheres (**B**), ChIP-seq signals for H3K27ac (green), H3K4me1 (gray), H3K4me3 (blue) at *Neurod2* gene were reduced by *Mll4* loss. ChIP-seq signals for MLL4 are shown for *Mll4*$^{f/f}$ cerebellum. Peak tracks in the BigBed format are shown as black lines (cerebellum) and blue lines (neurospheres) under the bottom of ChIP-seq tracks.

(**C** and **D**) A significant number of genes associated with super-enhancers (**C**) and broad H3K4me3 regions (**D**) were downregulated by *Mll4* loss. Genes (1,000) associated with super-enhancers or genes (1,000) associated with broad H3K4me3 were compared to genes upregulated (i.e., *Mll4* BSKO / *Mll4*$^{f/f}$ ≥ 2) or downregulated (i.e., *Mll4* BSKO / *Mll4*$^{f/f}$ ≤ 0.5) by *Mll4* loss. Gene expression analysis was performed using RNA-Seq data from 1-month-old cerebella. The *p* values were calculated using Fisher's exact test.

(**E**) Venn diagram showed that *Mll4*-loss-downregulated genes associated with super-enhancers highly overlapped with those associated with broad H3K4me3.

(**F and G**) Gene ontology analysis using DAVID showed that neuron differentiation genes were enriched in *Mll4*-loss-downregulated genes that were associated with super-enhancers (**F**) or broad H3K4me3 (**G**).

(**H and I**) Tumor suppressor genes were enriched in *Mll4*-loss-downregulated genes that were associated with super-enhancers (348 genes) (**H**) or broad H3K4me3 (332 genes) (**I**). The P values were calculated using Mann-Whitney Wilcoxon test.

Table S1

Table S1. A list of neuron-differentiation-relevant genes, tumor suppressor genes, and transcriptional repressor genes that are associated with super-enhancers and/or broad H3K4me3 (Transcriptional repressors are based on the information from http://www.cancer-genetics.org/index.htm), related to **Figures 3** and **7**

Gene	Super-enhancer	Broad H3K4me3	Neuron Differentiation
Adcy1	Y	Y	Y
Als2	Y	Y	Y
Atp2b2	Y	Y	Y
Boc	Y	Y	Y
En2	Y	Y	Y
Ephb2	Y	Y	Y
Gas7	Y	Y	Y
Lhx1	Y	Y	Y
Neurl1a	Y	Y	Y
Neurod2	Y	Y	Y
Nfib	Y	Y	Y
Nptx1	Y	Y	Y
Nrn1	Y	Y	Y
Ntrk3	Y	Y	Y
Rara	Y	Y	Y
Ski	Y	Y	Y
Srcin1	Y	Y	Y
Tlx3	Y	Y	Y
Uncx	Y	Y	Y

Gene	Super-enhancer	Broad H3K4me3	Tumor Suppressor	Repressor
Afap1l2	Y	N	Y	N
Amh	Y	Y	Y	N
Anp32a	Y	Y	N	Y
Bmf	Y	Y	Y	N
Bcl6	Y	Y	Y	Y
Cadm3	Y	Y	Y	N
Cbfa2t3	Y	Y	Y	Y
Dab2ip	Y	Y	Y	N
Dnmt3a	Y	Y	Y	Y
Dusp5	Y	Y	Y	N
Egr1	Y	Y	Y	N
Ephb2	N	Y	Y	N
Foxo3	Y	Y	Y	Y
Jup	Y	Y	Y	N
Lrrc4	Y	N	Y	N
Max	Y	Y	Y	Y
Mtus1	Y	N	Y	N
Mus81	Y	Y	Y	N
Mxi1	Y	N	Y	N
Ntrk3	N	Y	Y	N
Nuak1	Y	Y	Y	N
Pax6	Y	Y	Y	Y
Plcb3	Y	N	Y	N
Plekho1	Y	Y	Y	N
Ppp1r1b	Y	Y	Y	N
Ppp2r2c	Y	Y	Y	N
Tcf4	N	Y	Y	N
Trim3	Y	Y	Y	N
Trim62	Y	Y	Y	N
Zic1	Y	Y	Y	N